

Observation of back-action cancellation in interferometric and weak force measurements

T. Caniard, P. Verlot, T. Briant, P.-F. Cohadon, and A. Heidmann

Laboratoire Kastler Brossel, ENS, UPMC, CNRS; case 74, 4 place Jussieu, 75005 Paris, France

We experimentally demonstrate a cancellation of back-action noise in optical measurements. Back-action cancellation was first proposed within the framework of gravitational-wave detection by dual resonators as a way to drastically improve their sensitivity. We have developed an experiment based on a high-finesse Fabry-Perot cavity to study radiation-pressure effects in ultra-sensitive displacement measurements. Using an intensity-modulated intracavity field to mimic the quantum radiation-pressure noise, we report the first observation of back-action cancellation due to a destructive interference between radiation-pressure effects on both mirrors of the cavity. We have observed a sensitivity improvement by a factor larger than 20 both in displacement and weak force measurements.

Introduction.— The unique sensitivity of optical interferometry is used in many high-sensitivity measurements, including gravitational-wave interferometers [1, 2], optical transduction of the gravitational signal in Weber bars [3], monitoring of a micro-mechanical resonator [4, 5], or for weak force detection such as AFM [6]. Quantum noise of light however induces fundamental limits: current gravitational-wave interferometers are already confronted to the shot-noise limit at high frequency and the next generation of interferometers [7] and dual detectors with optical readout [8] will be confronted to the back-action noise through the radiation pressure on the test masses. A number of sophisticated quantum noise reduction schemes have been proposed to overcome the related *Standard Quantum Limit* (SQL): use of squeezed light sent into the interferometer [9, 10], use of quantum correlations induced by radiation pressure between phase and intensity fluctuations [11], quantum locking of mirrors [12] or detuning of the signal recycling cavity [13]. Recent results have also shown that the specific geometrical design of dual resonators [8] allows for their sensitivity to be strongly improved by a back-action noise cancellation effect, due to a destructive interference between radiation-pressure effects on both resonators [14].

We present in this paper the first experimental demonstration of such a back-action cancellation. We have developed an experiment to study radiation-pressure effects in a high-finesse Fabry-Perot cavity. A dual optical injection system allows us to mimic the quantum radiation-pressure noise by using a noisy classical intensity modulation [15]. We have observed a classical back-action cancellation and we demonstrate a drastic sensitivity improvement beyond the limit imposed by usual radiation-pressure noise, for the measurements of both a cavity length variation and of a weak force applied to one cavity mirror used as a mechanical transducer.

Back-action cancellation in a dual resonator sensor.— We consider a probe laser beam sent into a single-port lossless optical cavity. We study the response of the system to a variation δL_{sig} of the cavity length. The displacement fluctuations of the front and end mirrors are denoted δX_f and δX_e , respectively. The cavity length

fluctuations δL are then given by

$$\delta L = \delta X_e - \delta X_f + \delta L_{\text{sig}}. \quad (1)$$

We now determine the quantum-limited sensitivity of the optomechanical sensor in the measurement of δL_{sig} . When the cavity is at resonance, the fluctuations $\delta q^{\text{out}}[\Omega]$ of the phase quadrature of the reflected beam at a frequency Ω are given by [12]

$$\delta q^{\text{out}}[\Omega] = \delta q^{\text{in}}[\Omega] + \frac{16\mathcal{F}}{\lambda} \sqrt{I^{\text{in}}} \delta L[\Omega], \quad (2)$$

where λ is the laser wavelength, \mathcal{F} the cavity finesse, I^{in} the incident power (normalized as a photon flux), δq^{in} the phase-quadrature fluctuations of the incident beam, and we have assumed Ω much smaller than the cavity bandwidth.

Working at low temperature, the ultimate displacement noise is the back-action noise due to the radiation pressure exerted by the intracavity field on both mirrors: $F_{\text{rad}}(t) = 2\hbar k I(t)$, where $k = 2\pi/\lambda$ is the field wavevector and $I(t)$ the intracavity intensity. The response of the mirrors to radiation pressure is then described by linear response theory:

$$\delta X_e[\Omega] - \delta X_f[\Omega] = (\chi_e[\Omega] + \chi_f[\Omega]) F_{\text{rad}}[\Omega], \quad (3)$$

where χ_e and χ_f are the mirrors' mechanical susceptibilities. The sign change in the right-hand part of Eq. (3) is due to the opposite direction of the radiation-pressure force on both mirrors.

For a coherent state of light, the incident phase and intensity quadratures are uncorrelated and their noise spectra are normalized to 1. The sensitivity for a measurement of δL_{sig} therefore stems from a trade-off between phase and intensity noises. At low power, phase noise prevails and the sensitivity is given by $\delta L_{\text{shot}}[\Omega] = \lambda / (16\mathcal{F}\sqrt{I^{\text{in}}})$, whereas radiation-pressure effects prevail at higher power with a corresponding sensitivity

$$\delta L_{\text{ba}}[\Omega] = |\chi_e[\Omega] + \chi_f[\Omega]| \frac{4\hbar k \mathcal{F}}{\pi} \sqrt{I^{\text{in}}}. \quad (4)$$

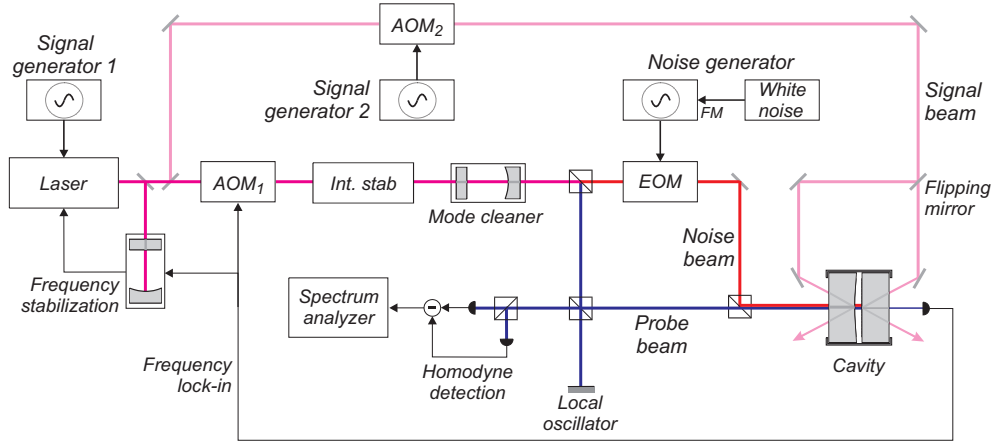


FIG. 1: Experimental setup. The high-finesse cavity is composed of two low-loss cylindrical mirrors. The frequency- and intensity-stabilized laser source is locked on the cavity resonance via an acousto-optic modulator (AOM₁). Two beams are sent into the cavity: a noise beam which is intensity-modulated by an electro-optic modulator (EOM) in order to apply a radiation-pressure noise on the mirrors, and a weaker probe beam whose reflected phase is measured by homodyne detection to monitor the mirror displacements. The signal in the measurement can either be an optical length variation of the cavity mimicked by a frequency modulation of the laser (signal generator 1), or a weak force applied through the radiation pressure of an intensity-modulated signal beam onto the front or end mirror of the cavity (signal generator 2). For simplicity, polarizing selective elements are not shown.

In the dual sphere antenna recently proposed for wide-band gravitational-wave detection [8], two spherical masses are nested together with only a small gap in-between whose length can be monitored by an optical cavity. The fundamental modes of both spheres have different resonant frequencies and their response to a gravitational wave are out-of-phase for intermediate frequencies: the global response is then enhanced when measuring the gap in-between. In contrast, as radiation-pressure forces have opposite directions, one gets a destructive interference between back-action effects on both resonators: the global back-action noise δL_{ba} is almost cancelled at the anti-resonance frequency Ω for which the sum $\chi_e + \chi_f$ vanishes. The measurement is then mainly limited by the shot noise δL_{shot} and the optimization of the incident light power leads to the sensitivity

$$\delta L_{min}[\Omega] = \sqrt{\hbar[\chi_e[\Omega] + \chi_f[\Omega]]}, \quad (5)$$

similar to a SQL sensitivity taking into account both resonators and their destructive interference. One then gets a drastic sensitivity improvement in the intermediate frequency band [14]: at the anti-resonance frequency, the real parts of the susceptibilities exactly compensate for each other, leaving only the imaginary part in expression (5). The sensitivity then reaches the ultimate quantum limit of the measurement [10].

Experimental setup.— Our experimental setup is based on a very-high finesse cavity made of two 1-inch high-quality cylindrical mirrors with very low losses: we have obtained a cavity finesse $\mathcal{F} = 230\,000$. The cavity is very short ($L = 0.25$ mm) in order to have a large cavity bandwidth ($\Omega_c/2\pi = 1.3$ MHz) and to reduce the influence of laser frequency noise. It is operated in vacuum to increase the mechanical quality factors.

The light beam entering the cavity is provided by a Ti:Sa laser working at 810 nm, frequency-stabilized on an external reference cavity. The light beam is also intensity-stabilized and spatially filtered by a mode cleaner. The phase fluctuations of the reflected beam are monitored by a homodyne detection. For an incident power of $50\,\mu\text{W}$, one gets a quantum-limited sensitivity of 2.7×10^{-20} m/ $\sqrt{\text{Hz}}$ at frequencies above 200 kHz.

In order to mimic the quantum fluctuations of radiation pressure, we have developed a dual-beam injection system: a second light beam (noise beam in Fig. 1, with a $300\,\mu\text{W}$ power, cross-polarized with the probe beam) is intensity-modulated with an electro-optic modulator (EOM) before entering the cavity to produce a classical intracavity radiation-pressure modulation. The EOM is driven by a high-frequency generator synchronized with the spectrum analyzer used in the homodyne detection, and frequency-modulated by a 600-Hz wide gaussian white noise. As compared to the 10-Hz resolution bandwidth of the spectrum analyzer, the resulting incident intensity fluctuations thus appear as a white noise which properly mimics -though at a higher level- the quantum fluctuations of the incident intensity.

As the experiment requires a perfect isolation of the phase of the probe beam with respect to the intensity of the noise beam, we have carefully eliminated unwanted optical reflections and residual birefringence of the high-finesse cavity. The optical rejection of the double-beam system is higher than 35 dB: in our experimental conditions, observable effects of the noise beam are therefore necessarily mediated by intracavity radiation pressure.

An additional intensity-modulated beam (signal beam in Fig. 1, with a 1 W power) can be used to apply a weak force ($\simeq 1$ nN) upon one of the mirrors through

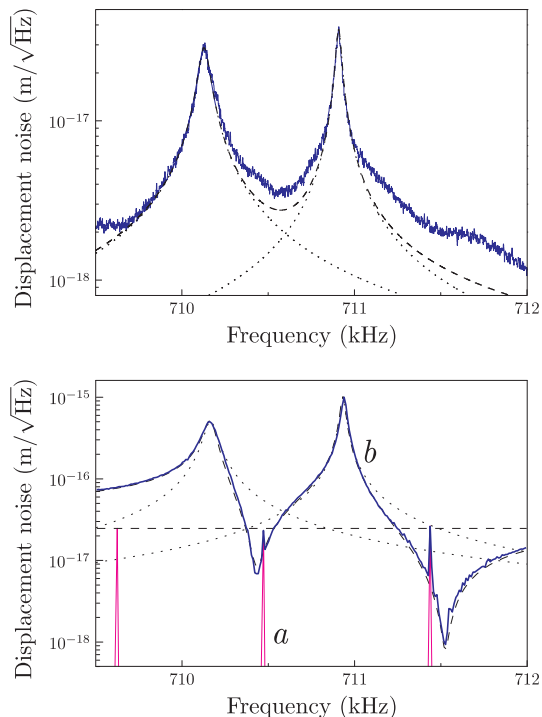


FIG. 2: Top: thermal noise spectrum of the cavity in the vicinity of a particular doublet. Each peak is related to a specific vibration mode of one mirror. The dashed line is a double Lorentzian fit corresponding to the quadratic sum of individual mirrors' thermal noises (dotted lines). Bottom: measurement of an optical length variation of the cavity produced by a modulation of the laser frequency. Curve *a* shows the monochromatic signal at different modulation frequencies, with the noise beam off. In presence of radiation-pressure noise (curve *b*), the signal is still observable in the dips associated with back-action cancellation. Dashed curves are theoretical fits of the signal and radiation-pressure noise, and dotted curves are the expected individual radiation-pressure noise spectra.

radiation pressure: a flipping mirror allows to actuate either the front or end mirror of the cavity. The beam spot can also be swept over the mirror surface in order to map the vibration profile of each mode [16].

Observation of radiation-pressure cancellation.— Cancellation effects are expected in our system since both mirrors have similar sizes and present acoustic modes at nearly equal resonance frequencies. The overall mechanical response thus appears as a set of resonant doublets. Near one particular doublet, the motion of each mirror is mainly ruled by its resonant mode, with a Lorentzian mechanical susceptibility given by

$$\chi_i[\Omega] = \frac{1}{M_i(\Omega_i^2 - \Omega^2 - i\Omega\Omega_i/Q_i)} + \chi_i^{(0)}, \quad (6)$$

where the index $i = \{e, f\}$ stands for the mirror, Ω_i is the resonance frequency of the mode, M_i its effective mass and Q_i its mechanical quality factor. The susceptibility $\chi_i^{(0)}$ describes the out-of-resonance response of all other mechanical modes of the mirror, assumed constant

near the doublet. Due to the geometry discrepancy, the two resonance frequencies Ω_i are slightly shifted. As the mechanical responses are out-of-phase for intermediate frequencies, one expects back-action cancellation in that frequency domain.

Figure 2 shows the thermal noise spectrum observed in the vicinity of a particular doublet. Since thermal noises of both mirrors are not correlated, their contributions are simply added as shown from the double Lorentzian fit. Excess noise is due to a neighboring doublet. We have checked by a selective optical actuation of each mirror that the lower-frequency resonance is due to the front mirror whereas the higher-frequency one is due to the end mirror. The fit yields the following parameters: $\Omega_f/2\pi = 710.1$ kHz, $\Omega_e/2\pi = 710.9$ kHz, $M_f = 0.64$ g, $M_e = 0.84$ g, $Q_f = 10\,500$, and $Q_e = 21\,500$. The discrepancy between the two effective masses M_f and M_e can be attributed to the different spatial overlap between the cavity field and the vibration modes [16].

We now turn the noise beam on and set its intensity-noise level in order for the mirror displacements induced by radiation pressure to be well above the thermal noise at every frequency. Curve *b* of Fig. 2 (bottom) shows the resulting mirror displacement spectrum, obtained by scanning the modulation frequency of the noise beam over the whole doublet, with a 10-Hz resolution bandwidth of the spectrum analyzer: one gets a clear cancellation of radiation-pressure effects between the two resonances as compared to the individual responses of each mirror (dotted lines deduced from the characteristics of the thermal noise spectra). The coherence between both radiation-pressure white noises driving the mirrors and their out-of-phase responses make them enter a 'common-mode' motion no longer observable by the probe beam. Back-action noise due to radiation pressure is then transferred to the common-mode motion. Another cancellation dip is observed at a higher frequency, where the out-of-phase response of the two resonant modes compensates the in-phase background response of all other modes.

To demonstrate the sensitivity improvement in length measurements, we generate a monochromatic modulation $\delta\nu_{\text{sig}}$ of the laser optical frequency ν , equivalent to an apparent variation δL_{sig} of the cavity length with $\delta L_{\text{sig}}/L = \delta\nu_{\text{sig}}/\nu$. Curve *a* of Fig. 2 (bottom) shows the effect of a small modulation, corresponding to optical length variations in the 10^{-17} m range, successively applied at different frequencies, with the noise beam off. In presence of radiation-pressure noise (curve *b*), the signal is no longer observed except at frequencies where back-action cancellation occurs. As compared to the individual radiation-pressure contributions (dotted lines), one gets a sensitivity improvement by a factor 25.

Weak-force sensitivity enhancement.— Back-action cancellation may also be useful to other optical measurements such as weak force detection [6]. For an optomechanical resonator used as a weak force sensor with a mechanical susceptibility $\chi[\Omega]$, the SQL of the displacement measurement leads to a related quantum limit for

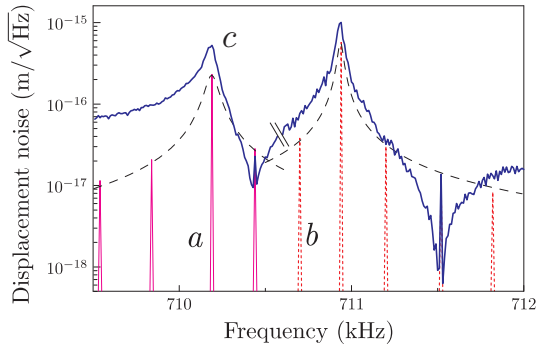


FIG. 3: Measurement of a weak force applied at different frequencies by the signal beam, either to the front (peaks *a* around the first resonance) or end (peaks *b* around the second resonance) mirror. Curve *c* is obtained in presence of radiation-pressure noise, with the force applied to the front mirror for frequency less than 710.6 kHz, and to the end mirror at higher frequency: the force is observable in the dips associated with back-action cancellation. Dashed curves are fits of both mirrors' dynamical responses to the force.

the force [17]

$$\delta F_{\text{SQL}}[\Omega] = \sqrt{\hbar/|\chi[\Omega]|}. \quad (7)$$

Consider now the sensor as the end mirror of a Fabry-Perot cavity (with $\chi = \chi_e$), with an almost identical one as front mirror. Since the latter is insensitive to the weak force, one can take advantage of the back-action cancellation inside the optical cavity to reach a sensitivity

$$\delta F_{\text{min}}[\Omega] = \frac{\sqrt{\hbar|\chi_e[\Omega] + \chi_f[\Omega]|}}{|\chi_e[\Omega]|}, \quad (8)$$

no longer limited by δF_{SQL} at anti-resonance frequencies.

As an illustration, we use our cavity to measure a weak force produced by the intensity-modulated signal beam.

This signal is set 5 dB below the back-action noise of the intracavity noise beam at the mechanical resonance frequency of the sensor. The frequency of the monochromatic force applied with the signal beam is scanned from 709.5 to 712 kHz: Fig. 3 shows the experimental spectra obtained with (curve *c*) and without (curves *a* and *b*) the noise beam, when the weak force is either applied onto the front (four first peaks) or end (five last peaks) mirror of the cavity. At the vicinity of back-action cancellation frequencies, curve *c* clearly shows that the weak force, otherwise unobservable, can be measured with a signal-to-noise ratio up to the order of 10.

Conclusion.— We have demonstrated classical back-action cancellation, which can be considered as a proof-of-principle demonstration of quantum back-action cancellation [14] as quantum-limited interferometry can be understood in purely classical terms [15]. Though classical intracavity radiation-pressure effects have already been demonstrated with specially designed mirrors [18, 19] or suspended mirrors [20], this is the first demonstration of such effects with the much stiffer resonators provided by the internal vibration modes of standard fused silica mirrors. The correlations between the phase of the probe beam and the intensity of the noise beam could be extended to the quantum level by further experimental progress and cryogenic operation of the cavity, allowing for radiation-pressure induced QND measurement of light intensity [21] and other quantum optics experiments.

We gratefully acknowledge Jean-Marie Mackowski and his group at the Laboratoire des Matériaux Avancés for the optical coating of the low-loss mirrors. This work was partially funded by EGO (collaboration convention EGO-DIR-150/2003 for a study of quantum noises in gravitational wave interferometers) and by the Integrated Large Infrastructures for Astroparticle Science (ILIAS) of the Sixth Framework Program of the European Community.

-
- [1] C. Bradaschia *et al.*, Nucl. Inst. Meth. Phys. Res. A **289**, 518 (1990).
 - [2] A. Abramovici *et al.*, Science **256**, 325 (1992).
 - [3] L. Conti, M. De Rosa, F. Marin, L. Taffarelli, and M. Cerdonio, J. Appl. Phys. **93**, 3589 (2003).
 - [4] O. Arcizet *et al.*, Phys. Rev. Lett. **97**, 133601 (2006).
 - [5] H. R. Böhm *et al.*, Appl. Phys. Lett. **89**, 223101 (2006).
 - [6] D. Rugar, R. Budakian, H.J. Mamin, and B.W. Chui, Nature **430**, 329 (2004).
 - [7] G.M. Harry, J.L. Houser, and K.A. Strain, Phys. Rev. D **65**, 082001 (2002).
 - [8] M. Cerdonio *et al.*, Phys. Rev. Lett. **87**, 031101 (2001).
 - [9] C.M. Caves, Phys. Rev. D **23**, 1693 (1981).
 - [10] M.T. Jaekel and S. Reynaud, Europhys. Lett. **13**, 301 (1990).
 - [11] H.J. Kimble *et al.*, Phys. Rev. D **65**, 022002 (2002).
 - [12] J.-M. Courty, A. Heidmann, and M. Pinard, Phys. Rev. Lett. **90**, 083601 (2003).
 - [13] A. Buonanno and Y. Chen, Phys. Rev. D **64**, 042006 (2001).
 - [14] T. Briant *et al.*, Phys. Rev. D **67**, 102005 (2003).
 - [15] C.M. Mow-Lowry *et al.*, Phys. Rev. Lett. **92**, 161102 (2004).
 - [16] T. Briant, P.-F. Cohadon, A. Heidmann, and M. Pinard, Phys. Rev. A **68**, 033823 (2003).
 - [17] R. Fermani, S. Mancini, and P. Tombesi, Phys. Rev. A **70**, 045801 (2004).
 - [18] B.S. Sheard *et al.*, Phys. Rev. A **69**, 051801(R) (2004).
 - [19] O. Arcizet, P.-F. Cohadon, T. Briant, M. Pinard, and A. Heidmann, Nature **444**, 71 (2006).
 - [20] T. Corbitt, D. Ottaway, E. Innerhofer, J. Pelc, and N. Mavalvala, Phys. Rev. A **74**, 021802(R) (2006).
 - [21] A. Heidmann, Y. Hadjar, and M. Pinard, Appl. Phys. B **64**, 173 (1997).